International Journal of Civil Engineering (IJCE)
ISSN(P): 2278-9987; ISSN(E): 2278-9995
Vol. 3, Issue 1, Jan 2014, 59-66

International Academy of Science, Engineering and Technology
Connecting Researchers; Nurturing Innovations

HYDROTHERMAL MAPPING OF MARU SCHIST BELT, NORTH-WESTERN NIGERIA USING REMOTE SENSING TECHNIQUE

KUDAMNYA E. A[1], ANDONGMA W. T[2] & OSUMEJE J. O[3]

[1,2]Department of Geology, Ahmadu Bello University, Zaria, Kaduna, Nigeria

[3]Department of Physics, Ahmadu Bello University, Zaria, Kaduna, Nigeria

ABSTRACT

Mineral deposits are well known to be associated with hydrothermal alteration. In north-western Nigeria however, the Maru schist belt is known to be endowed with iron mineralization occurring as Banded Iron Formation (BIF). Land sat Enhanced Thematic Mapper (ETM+) data of the study area were evaluated using colour composite Images produced for lithological mapping in order to identify the alteration zones.

The technique employed in the processing of hydrothermal alterated zones for these imageries is band ratio. This includes the use of Chica – Olma ratio, Abrams ratio and Kauffmann ratio. As a result, iron oxides and hydroxyl minerals were detected in the area. Some ratio images were displayed in gray tones in order to show the extent of alteration within this schist belt. False color composite was also used for lithologic mapping of the different rock type in the area. A new geological map was generated and compared to an already published map of the study area. Comparison between the different band ratios techniques show a close correlation between iron altered zones which are also well known for Iron mineralisation.

The results show that the band rationing technique proved to be effective in mapping zones of mineralisation. It is therefore concluded that the remote sensing technique can be applied for lithologic and hydrothermal alteration mapping within the Maru schist belt, Northwest Nigeria.

KEYWORDS: Banded Iron Formation, Band Ratio, False Colour Composite, Hydrothermal Alteration, Schist Belt

INTRODUCTION

Mineral deposits are well known to be associated with hydrothermal alteration. Beane (1982) defined hydrothermal alteration as the reflection of response from pre-existing rock-forming minerals to physical and chemical conditions different than those, under which they originally formed, especially by the action of hydrothermal fluids. The hydrothermal fluid processes alter the mineralogy and chemistry of the host rocks that can produce distinctive mineral assemblages which vary according to the location, degree and duration of those alteration processes. When these alteration products are exposed at the surface, they can be mapped as a zonal pattern.

The importance of the recognition of such spatial patterns of alteration makes the ‘remote sensing technique’ one of the standard procedures in exploration geology, due to its high efficiency and low cost (Yetkin, 2003). Many studies around the world related to hydrothermal alteration mapping have used multispectral satellite images especially Land sat and Aster (Abdelsalam *et al.,* 2000; Ramadan *et al.,* 2001; Madani *et al.,* 2003; Ramadan and Kontny, 2004). Also, in mining exploration, satellite images have been widely used to identify hydrothermally altered areas and to identify faults and areas of mineralization (Goetz and Rowan, 1983; Kauffmann 1988; Crosta and Moore 1989; Loughlin 1991; Wester, 1992; Van der Meer et al., 1995).

According to Ibrahim (2012), the schist belts occur in a 300 to 400 km wide zone, predominantly west of longitude 8^{o}E, trending NNE, and can be traced along strike for about 800 km. They are apparently infolded into the Migmatite-Gneiss Complex. The Schist Belts comprise low grade, metasediment-dominated belts trending N–S which are best developed in the western half of Nigeria, shown in Figure 1.

In north-western Nigeria however, the Maru schist belt is known to be endowed with iron mineralization occurring as Banded Iron Formation (BIF). Also, Obaje (2009); and Ibrahim (2012) reports that Maru schist belt is characterized by the dominance of pelitic rocks occurring mainly as phyllites and slates interlaminated with siltstones, banded iron formation (BIF) containing magnetite, hematite and garnet, calc-silicate rocks and marbles as well as basic to acid meta -volcanics are also present.

This study is aimed at mapping the hydrothermal altered minerals within and around the Maru schist belt in order to establish zone of Iron (Fe) and clay enrichment, using information obtained via satellite imagery using conventional methods of colour composites, band ratio, Crosta technique. Bands 1 – 7 of Enhanced Thematic mapper plus (ETM+) acquired on April 17, 2000. It has data scenes number 190/051(Path/Row).

LOCATION AND GEOLOGY OF THE STUDY AREA

The study area lies within Zamfara State of the north-western basement complex of northern Nigeria. These belts are considered to be Upper Proterozoic supracrustal rocks which have been infolded into the migmatite-gneiss-quartzite complex. The lithological variations of the schist belts include coarse to fine grained clastics, pelitic schists, phyllites, banded iron formation, carbonate rocks (marbles/dolomitic marbles) and mafic metavolcanics (amphibolites). Some may include fragments of ocean floor material from small back-arc basins.

The schists may also contain graphite, magnetite and pyrite in several localities especially in the south east (Egbuniwe, 1982). The fine-grained laminated sediments, both pelites and iron formation, indicate quiet water conditions; the predominance of iron oxides suggests oxygenated waters, although sometimes pyrite occurs, indicating anoxic conditions. Metasandstones were deposited in a higher energy environment, reflecting shallow water conditions or increased sediment supply.

Rahaman (1976) and Grant (1978) suggested that there were several basins of deposition whereas Oyawoye (1972) and McCurry (1976) consider the schists belts as relicts of a single supracrustal cover. Olade and Elueze (1979) consider the schist belts to be fault-controlled rift-like structures. Grant (1978), Holt (1982) and Turner (1983), based on structural and lithological associations, suggest that there are different ages of sediments. However, Ajibade et al. (1979) disagree with this conclusion and show that both series contained identical deformational histories. The structural relationships between the schist belts and the basement were considered by Trus well and Cope (1963) to be conformable metamorphic fronts and it was Ajibade et al. (1979) who first mapped a structural break.

In the Maru belt, pelitic rocks are dominant, mainly as phyllites and slates interlaminated with siltstones. Banded iron formation (BIF), containing magnetite, hematite and garnet is also present. Impure micaceous quartzites occur near the eastern margin of the belt. Mafic volcanic rocks are represented by the amphibolites at several localities. The Maru Schist Belt also contains internal plutons of granite, granodiorite and syenite.

They show little of the complexicity and variable fold trends. It is a straight NNE-trending belt with a steeply dipping foliation which is axial planar to tight folds and deformed by later crenulation cleavages. Kibaran ages have been estimated for the Maru Schist Belt.

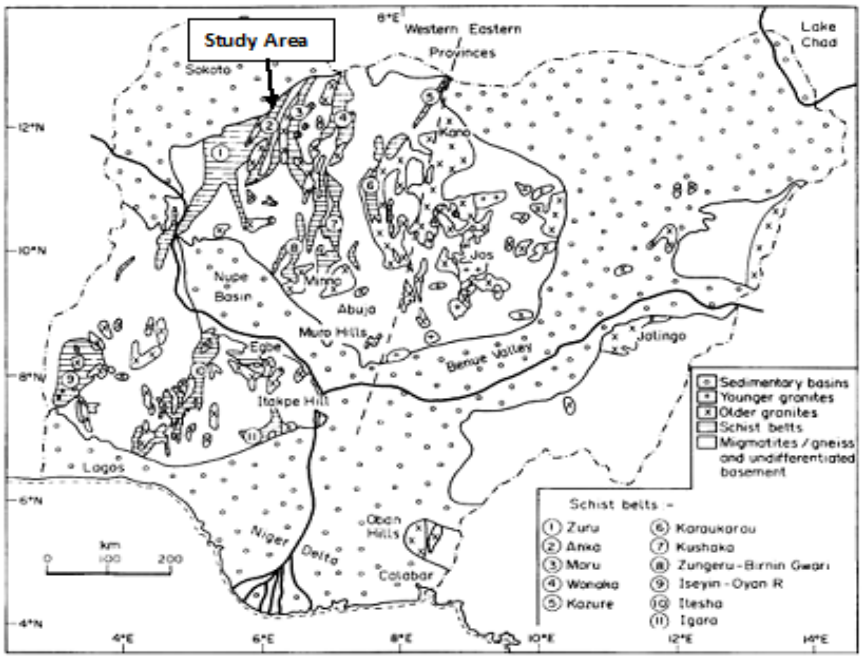

Figure 1: Geological Map of Nigeria Showing the Location of the Study Area

METHODOLOGY

The methodology employed involves the use of land satellite imageries, obtained for bands 1-7 enhanced themetic mapper-plus (ETM+) data (190/051 path/row, with acquisition date 27 June, 2000) of the Maru area, for the study. These imageries were processed using remote sensing software ENVI 4.5 to form colour composite images, by assigning bands 7, 4, 1 to the red, green and blue channels (RGB) respectively producing false colour composite (FCC) image used for lithologic mapping.

This was followed by production of band ratio imageries, where one band was divided on another based on their spectral response. Mathematically, band rationing is expressed as;

$$BV_{i,j,r} = \frac{BV_{i,j,k}}{BV_{i,j,l}}$$

Where; $BV_{i,j,r}$ is the output ratio for the pixel at row i and column j; $BV_{i,j,k}$ is the brightness value at the same location in band k, and $BV_{i,j,l}$ is the brightness value in band L.

The range of $BV_{i,j,r}$ is from 0 to 255 digital numbers (DN). The resulting ratio matrix is encoded to a standard 8-bit format by the help of normalizing functions like linear stretching.

The process was then repeated for two additional sets of bands. Combination into red, green and blue channel to produce a false colour composite of these ratio imageries were obtained using the following band ratio: Chica – Olma ratio, Kauffmann ratio and Abrams ratio.

With the Chica – Olma ratio technique, the band ratios 5/7:5/4:3/1 were obtained and assigned the red, green and blue channels respectively to produce a false colour composite. Similarly band ratios 5/7:3/2:4/5 was obtained for Abrams ratio technique while 7/4:4/3:5/7 for Kauffmann ratio technique. Both in each case (Abrams and Kauffmann's ratio techniques), the ratio imageries were assigned to the red, green and blue channels respectively.

Results of the combined imageries obtained using the Chica – Olma ratio technique, Abrams ratio technique and Kauffmann ratio technique were compared with one another, and subsequently with map of previous studies in the area.

RESULTS AND DICUSSIONS

Results from the individual band ratio images, it was observed that band ratio 5/7 displayed hydrothermally altered clay minerals as light tone, while the band ratio 5/4 and 3/1 each display ferrous and ferric iron minerals as light tones. This was shown respectively in the Figure 2 B, C and D. Band ratio 5/7 displayed light tones for clay minerals because the clay minerals have highest reflectance in band 5 and lowest reflectance/absorption in band 7. Similarly, ferrous (Fe^{2+}) and ferric (Fe^{3+}) iron minerals have highest reflectance on band 5 and 3 and lowest reflectance on bands 4 and 1 respectively. Thus, areas within the banded iron formation (BIF) can be distinguished on the basis of their ferrous and ferric iron bearing mineral potentials.

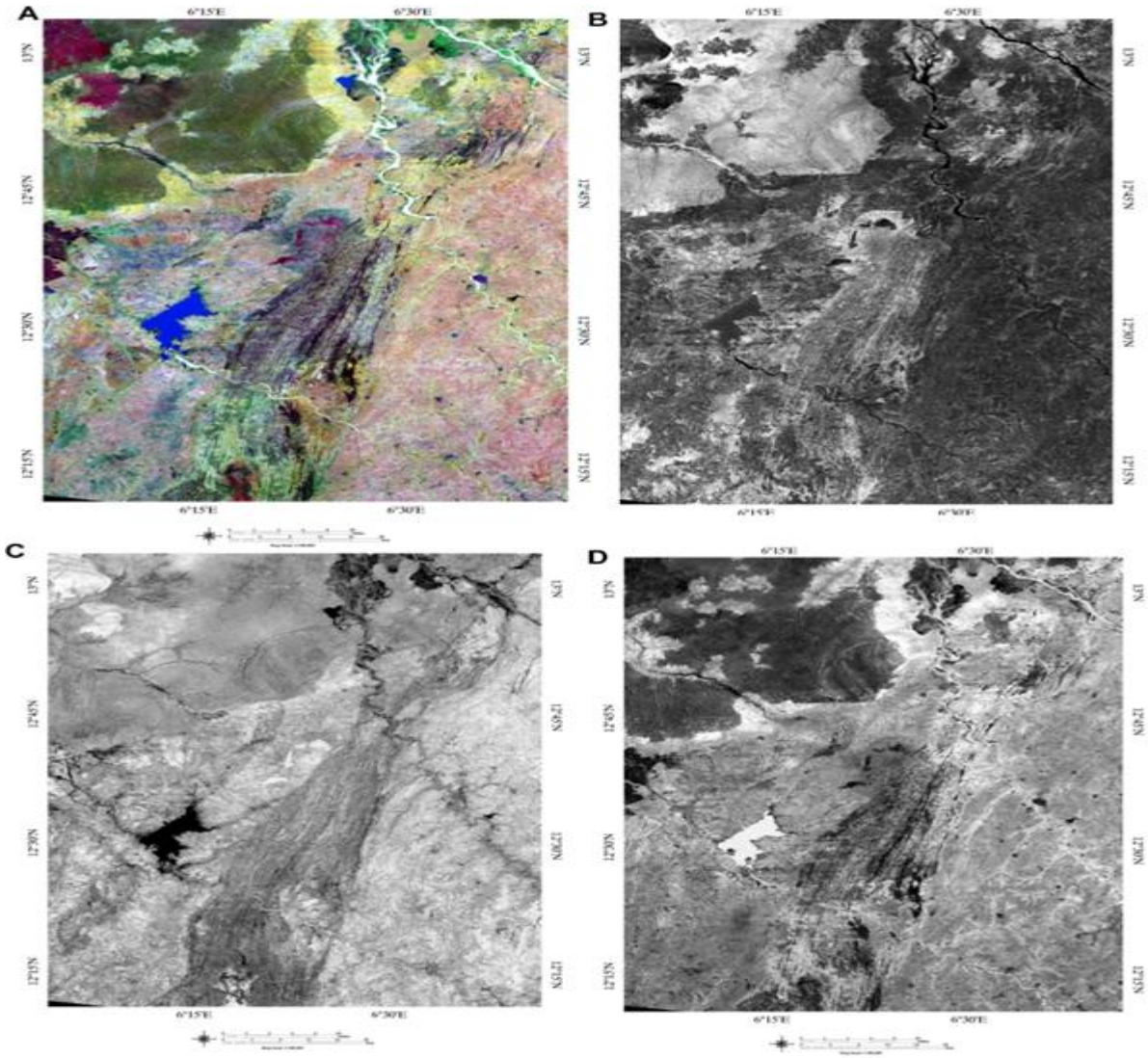

Figure 2: (a) Band 7, 4, 1 False Colour Composite of Study Area Showing Sans Tone as Dark Green, Alluvial as Yellow, Granitoids as Pink and Metase Diments/BIF as Puple
(b) Band Ratio 5/7 Image Displaying Clay Mineral Alteration as Light Tone
(c) Band Ratio 5/4 Image Displaying Iron Alteration as Light Tone
(d) Band Ratio 3/1 Image Displaying Iron Alteration as Light Tone

Lithologic mapping with false colour composite images displayed sandstone as green colour, granitoids as pink alluvial as yellow and metasedimentary/BIF rocks were displayed as dark to light pink Figure 2A.

The Chica-Olma ratio (5/7:5/4:3/1), enhances a hydrothermally altered clay minerals as red, ferrous iron as green and ferric iron as blue, shown in Figure 3.

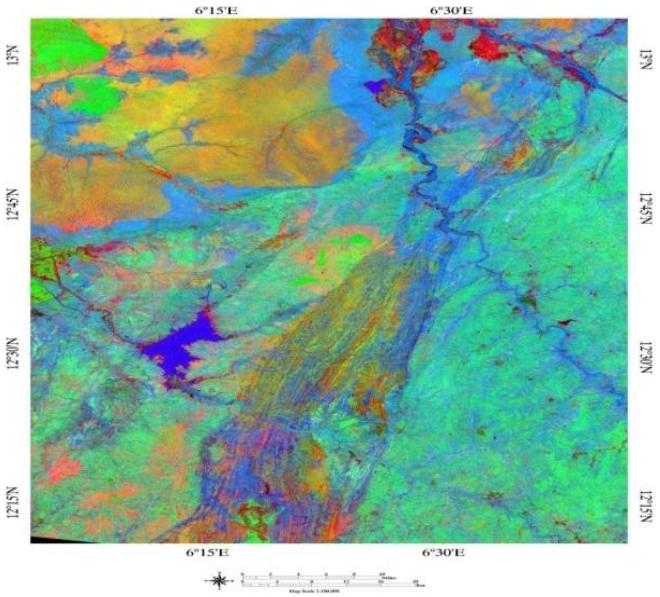

Figure 3: Chica-Olma Ratio Image (5/7, 5/4, 3/1), Displaying Altered Clay Minerals as Red, Ferrous (Fe^{2+}) Iron as Green and Ferric (Fe^{3+}) Iron as Blue

Using Kaufmann ratio (7/4:4/3:5/7), Iron minerals are displayed as red and hydroxyl minerals are displayed as blue, green pixels represents vegetation Figure 4. However, the use of Abrams ratio (5/7:3/2:4/5) helps to enhance hydrothermally altered clay minerals as red and iron oxide as green. Clay and iron dominated areas are displayed as blue pixels. Dark blue pixels representing areas more enriched in FeO Figure 5.

This provides an exact and more updated match when lithologic map was drawn from satellite image and compared to pre-existing map, shown in Figure 6A and B below. On the basis of their wavelength values within the electro-magnetic spectrum of light, band ratios 1.65/2.2 µm, 0.66/0.56 µm and 0.83/1.65 µm corresponds to the ratios band 5/band 7, band 3/band 2 and band 4/band 5 (Amera, 2007; and Yetkin, 2003).

These ratios were selected for the red, green and blue channels respectively. Thus, it reveals that Iron oxide-rich areas are displayed as green due to the presence of ferric iron charge transfer band in the ultraviolet region of the spectrum. Clay-rich areas are displayed as red, due to the presence of the hydrous minerals absorption band near 2.2 µm. Yellow or orange areas represent the areas where both clay and iron oxide minerals are present

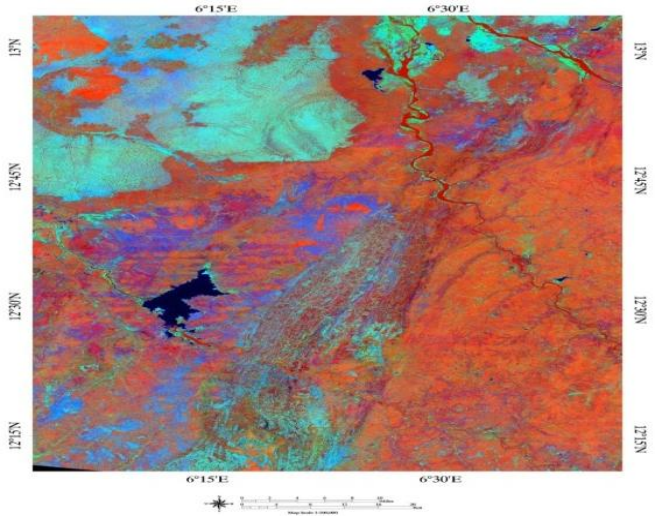

Figure 4: Kauffmann Ratio Image (7/4:4/3:5/7), Displaying Iron Minerals as Red, Hydroxyl Minerals S Blue and Background Areas as Green

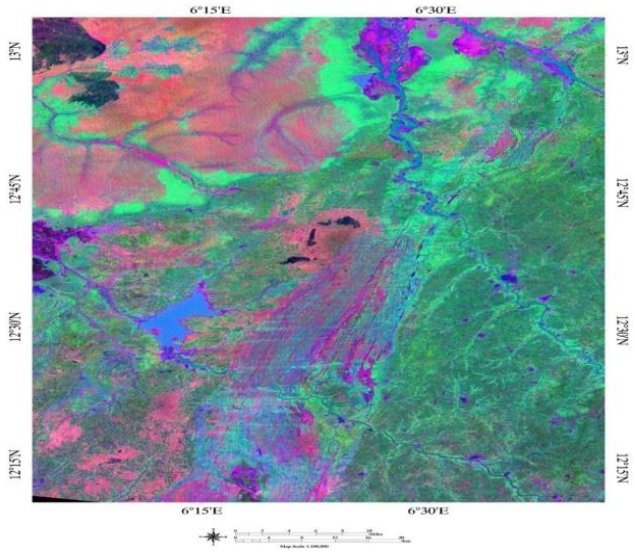

Figure 5: Abrams Ratio Image (5/7:3/2:4/5), Displaying Hydrothermally Altered Clay Minerals as Red and Iron Oxide as Green Blue Represent Areas with Both Clay and Iron Mineral Alteration

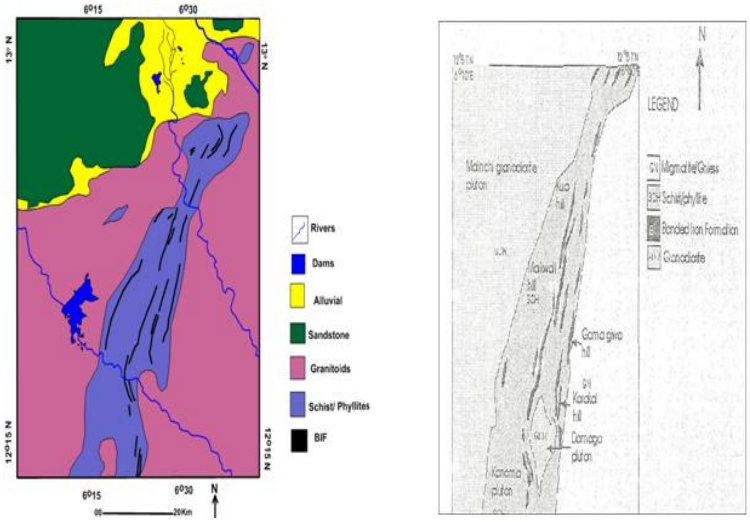

Figure 6: Geologic Map of Maru Schist Belt (a) Drawn from Satellite Imagery (b) Drawn from Satellite Imagery (Ibrahim 2012)

CONCLUSIONS

It can be concluded that remote sensing especially the band ratio techniques provide a fast and reliable means of mapping hydrothermal and iron mineralization within the Maru Schist belt. This was verified beyond reasonable doubt, as the remote sensing technique employed in the study matches with previous geologic mapping of banded iron formation and further updates lithologic and mineral information in this area. Correlation between the Chica-Olma ratio, the Abrams ratio and Kauffmann ratio images also prove the reliability of this method for exploration of iron mineralization within this schist belt. Using false colour composite image a distinction between major lithologies outcropping within this schist belt can be mapped effectively.

ACKNOWLEDGEMENTS

We thank the Global Land Cover Facility (GLCF), University of Maryland, College Park, U. S. A., for making available on the internet, remotely sensed Enhanced Thematic Data plus (ETM+) satellite data used for the analysis.

REFERENCES

1. **Abdelsalam, M. G., Stern, R. J. and Berhane, W. G., (2000).** Mapping gossans in arid regions with Landsat TM and SIR-C images: The Beddaho alteration zone in northern Eritrea; *J. African Earth Sci.* 30(4): pp. 903–916.
2. **Ajibade, A.C., Fitches, W. R., Wright, J. B., (1979).** The Zungeru mylonites, Nigeria: Recognition of a major unit. Rev de Geol Geog Phys 21: pp. 359–363.
3. **Amera, S. A., (2007).** Spectral remote sensing of hydrothermal alteration associated with volcanogenic massive sulphide deposits, Gorob-Hope Area, Namibia. A M Sc. thesis submitted to the International Institute for Geo-Information Science and Earth Observation.
4. **Beane, R. E., (1982).** Hydrothermal alteration in silicate rocks, southwestern North America in Titley, S. R., ed., *Advances in Geology of the Porphyry Copper Deposits, South-western, North America:* Tucson, Univ. Ariz. Press, Chapter 6.
5. **Crosta, A., Moore, J McM (1989).** Enhancement of Landsat Thematic Mapper imagery for residual soil mapping in SW Minais Gerais State, Brazil: A prospecting case history in Greenstone belt terrain; *International Proceedings of the Seventh Erim Thematic Conference: Remote Sensing for Exploration Geology*, pp. 1173–1187.
6. **Egbuniwe, I. G., (1982).** Geotetonic Evolution of the Maru belt, northwestern Nigeria. Ph.D thesis, University of Wales, Aberystwyth, U.K.
7. **Goetz, A. F., Rock, F. H., and Rowan, B. N., (1983).** Remote sensing for exploration: An overview; Eco. Geol. 78: pp. 573–590.
8. **Grant, N. K., (1978).** Structural distinction between a metasedimentary cover and an underlying basement in the 600 my old Pan-African domain of Northwestern Nigeria. *Geol Soc. Am. Bull.* 89: pp. 50–58.
9. **Holt, R. W., (1982).** The Geotectonic Evolution of the Anka Belt in the Precambrian Basement Complex of N.W. Nigeria. Unpublished Ph.D. Thesis, the Open University.
10. **Ibrahim A.A., (2012).** Formation of Atoll Garnets in the Banded Iron Formation of Maru Schist Belt, *American International Journal of Contemporary Research*, Vol. 2 No. 5.
11. **Kaufman, H., (1988).** Mineral exploration along the Agaba Levant structure by use of TM-data concepts, processing and results. *International Journal of Remote Sensing* 9: pp1630-1658.
12. **Loughlin, W. P., (1991).** Principal component analysis for alteration mapping, *Journal Photogrammetric Engineering and Remote Sensing* 57: pp 1163–1169.
13. **Madani, A., Abdel-Rahman, E. M., Fawzy, K. M., and Emam, A., (2003).** Mapping of the hydro- thermal alteration zones at Haimur Gold Mine Area, South Eastern Desert, Egypt using remote sensing techniques; *The Egyptian J. Rem.Sens. Space Sci*. 6: pp.47-60.
14. **McCurry, P., (1976).** Geology of the Precambrian to Lower Paleozoic rocks of northern Nigeria – A Review. In:C.A Kogbe (Ed.) *Geology of Nigeria* pp.15 – 39. Elizabethan Publication, Lagos.
15. **Obaje, N. G., (2009).** *Geology and mineral resources of Nigeria, lecture notes in earth science*.

16. **Olade, M. A., Elueze, A. A., (1979).** Petrochemistry of the Ilesha amphibolite and Precambrian crustal evolution in the Pan-African domain of SW Nigeria. Precambrian Res 8: pp.303-318.

17. **Oyawoye, M. O., (1972).** The basement complex of Nigeria. In: Dessauvagie TFJ, Whiteman AJ (eds) *African geology*. Ibadan University Press, pp 66–102.

18. **Rahaman, M.A., (1976).** Review of the basement geology of South-Western Nigeria. In: Kogbe C. A. (ed) *Geology of Nigeria*, 2nd edn, Elizabethan Publishers, Lagos, pp 41–58.

19. **Ramadan, T. M., and Kontny, A., (2004).** Mineralogical and structural characterization of alteration zones detected by orbital remote sensing at Shalatein District, SE Desert, Egypt; *J. African Earth Sci.* 40 89–99.

20. **Ramadan. T. M., Abdelsalam, M. G., and Stern, R. J., (2001).** Mapping gold-bearing massive sulfide deposits in the neoproterozoic Allaqi Suture, Southeast Egypt with Landsat TM and SIR-C/X SAR images; Photogrammetric Eng. Rem.Sens. 67(4) 491–497.

21. **Truswell, J. F., and Cope, R. N., (1963).** The geology of parts of Niger and Zaria provinces, Northern Nigeria: *Geol. Surv. Nigeria, Bull*. no. 29.

22. **Turner, D. C., (1983).** Upper Proterozoic Schist belts in the Nigerian sector of the Pan – African Province of West Africa. *Precambrian Research* 21: pp. 55–79.

23. **Wester, K., (1992).** Spectral signature measurements and image processing for geological remote sensing: Ph.D Thesis, Department of Physical Geography, Stockholm University, Stockholm, 130 p.

24. **Yetkin, E., (2003).** Alteration mapping by remote sensing: Application to Hasandağ– Melendiz Volcanic Complex: A M Sc. thesis submitted to the Graduate school of Natural and Applied Sciences of the Middle East Technical University.